Toxicology in Vitro 23 (2009) 808–815

Contents lists available at ScienceDirect

Toxicology in Vitro

journal homepage: www.elsevier.com/locate/toxinvit

Oxidative stress contributes to silica nanoparticle-induced cytotoxicity in human embryonic kidney cells

Fen Wang [a], Feng Gao [a,*], Minbo Lan [b], Huihui Yuan [b], Yongping Huang [c], Jianwen Liu [c]

[a] Department of Pharmaceutics, School of Pharmacy, East China University of Science and Technology, 130 Meilong Road, Shanghai 200237, China
[b] Testing Information Analysis Center, East China University of Science and Technology, Shanghai 200237, China
[c] Department of Pharmacological, School of Pharmacy, East China University of Science and Technology, Shanghai 200237, China

ARTICLE INFO

Article history:
Received 10 December 2008
Accepted 20 April 2009
Available online 3 May 2009

Keywords:
Silica nanoparticles
Cytotoxicity
Oxidative stress

ABSTRACT

In order to elucidate the nanoparticle-induced cytotoxicity and its mechanism, the effects of 20 and 50 nm silica nanoparticles on cultured human embryonic kidney (HEK293) cells were investigated. Cell viability, mitochondrial function, cell morphology, reactive oxygen species (ROS), glutathione (GSH), thiobarbituric acid reactive substance (TBARS), cell cycle and apoptosis were assessed under control and silica exposed conditions. Exposure to 20 or 50 nm SiO_2 nanoparticles at dosage levels between 20 and 100 μg/ml decreased cell viability in a dose-dependent manner. Median lethal dose (LD_{50}) of 24 h exposure was 80.2 ± 6.4 and 140.3 ± 8.6 μg/ml for 20 and 50 nm SiO_2 nanoparticles, respectively. Morphological examination revealed cell shrinkage and nuclear condensation after SiO_2 nanoparticle exposure. Increase in intracellular ROS level and reduction in GSH content were also observed in SiO_2 nanoparticle-exposed HEK293 cells. Increase in the amount of TBARS suggested an elevated level of lipid peroxidation. Flow cytometric analysis showed that SiO_2 nanoparticles can cause *G2/M* phase arrest and apoptotic sub-*G1* population increase in a dose-dependent manner. In summary, exposure to SiO_2 nanoparticles resulted in a dose-dependent cytotoxicity in cultured HEK293 cells that was associated with increased oxidative stress.

1. Introduction

Nanomaterials are commonly defined as materials having at least one dimension of less than 100 nm. Due to their unique physical and chemical characteristics, nanotechnology has become one of the leading technologies over the past 10 years. There is enormous interest in applying nanomaterials in a variety of industries. As a non-metal oxide, silica (SiO_2) nanoparticles have been found extensive applications in chemical mechanical polishing and as additives to drugs, cosmetics, printer toners, varnishes and food. In recent years, the use of SiO_2 nanoparticles has been extended to biomedical and biotechnological fields, such as biosensors for simultaneous assay of glucose, lactate, L-glutamate, and hypoxanthine levels in rat striatum (Zhang et al., 2004), biomarkers for leukemia cell identification using optical microscopy imaging (Santra et al., 2001), cancer therapy (Hirsch et al., 2003), DNA delivery (Bharali et al., 2005; Gemeinhart et al., 2005), drug delivery (Slowing et al., 2008), and enzyme immobilization (Barik et al., 2008).

Although nanomaterials are currently being widely used in modern technology, there is a lack of information regarding the health and environmental implications of manufactured nanomaterials to human. Studies on biological-effects of nanomaterials were mainly focused on cardiopulmonary toxicology of nano-titania, SiO_2, carbon nanotubes, fullerenes C60, and nano-iron (Pisanic et al., 2007; Warheit et al., 2007; Wick et al., 2007; Komatsu et al., 2008). Recently, data on SiO_2 nanoparticle-induced oxidative stress and proinflammatory responses in rodent and RAW264.7 cell line were published (Park and Park, 2008). For example, it was found that SiO_2 nanoparticles induced oxidative stress, proinflammatory stimulation, and aberrant clusters of topoisomerase I in the nucleoplasm in cells, fibrogenesis in Wistar rats (Peters et al., 2004; Chen and von Mikecz, 2005; Arts et al., 2007). Silica nanoparticles also showed oxidative stress-induced cytotoxicity in different types of cultured mammalian cell lines (Lin et al., 2006; Chang et al., 2007). Oxidative stress is the result of an imbalance in the pro-oxidant/antioxidant homeostasis. Various reactive oxygen

Abbreviations: BHT, butylated hydroxytoluene; DCF, dichlorofluorescein; DCFH–DA, 2′,7′-dichlorofluorescin diacetate; DMEM, Dulbecco's modified Eagle's medium; DMSO, dimethyl sulfoxide; FBS, fetal bovine serum; GSH, glutathione; HEK293, human embryonic kidney cell line; LD_{50}, median lethal dose; MDA, malondialdehyde; MTT, 3-(4,5-dimethylthiazol-2-yl)-2,5-diphenyltetrazolium bromide; PBS, phosphate buffered saline; ROS, reactive oxygen species; SiO_2, silica; TBA, 2-thiobarbituric acid; TBARS, thiobarbituric acid reactive substance.

* Corresponding author. Tel.: +86 21 6425 2449; fax: +86 21 6425 8277.
E-mail address: fgao@ecust.edu.cn (F. Gao).

0887-2333/$ - see front matter Crown Copyright © 2009 Published by Elsevier Ltd. All rights reserved.
doi:10.1016/j.tiv.2009.04.009

species (ROS), such as superoxide, hydrogen peroxide, hydroxyl and other oxygen radicals, are involved in oxidative stress. There has been an increase in biochemical, clinical, and epidemiological evidences that indicate the involvement of oxidative stress in various diseases, cancer, and aging (Yoshida et al., 2004; Mitsikosta et al., 2008). Our previous study in rodent observed a methotrexate-induced intestinal damage closely related to the increase in ROS (Gao and Horie, 2002; Miyazono et al., 2004).

It is possible that the inhaled nanoparticles penetrate the lungs and become deposit in the extra-pulmonary tissues. Inhaled ambient ultrafine particles can be found in heart, bone marrow, liver, kidney, and even central nervous system (Kreyling et al., 2002; Nemmar et al., 2004; Chen et al., 2006; Kleinman et al., 2008). Although the toxicity of nanoparticles on extra-pulmonary tissues has gradually drawn attention, it has rarely been reported. Thus, the potential toxic effects of SiO_2 nanoparticles on human health and the mechanisms underlining the processes warrant further studies.

The human embryonic kidney cell line (HEK293) was selected in the present study as an in vitro model to assess cytotoxicity and the eventuality of kidney toxicity. This cell line has been well characterized for its relevance to the toxicity models in human (Florea et al., 2007; Ji et al., 2008). To elucidate the possible mechanisms of cytotoxicity, a variety of surrogate parameters including cellular morphology, cell viability, mitochondrial function (MTT assay), reactive oxygen species (ROS), reduced glutathione (GSH), and thiobarbituric acid reactive substance (TBARS), levels was quantitatively assessed and compared between controls and SiO_2 nanoparticle treated groups. Furthermore, the effects of SiO_2 nanoparticles in inducing apoptosis in HEK293 cells were studied.

2. Materials and methods

2.1. Chemicals

Dulbecco's modified eagle's medium (DMEM), penicillin, streptomycin and fetal bovine serum (FBS) were purchase from Invitrogen (Carlsbad, CA, USA). 3-(4,5-Dimethylthiazol-2-yl)-2,5-diphenyltetrazolium bromide (MTT), Triton X-100, propidium iodide, RNase A, 2′,7′-dichlorofluorescin diacetate (DCFH–DA), 2-thiobarbituric acid (TBA), butylated hydroxytoluene (BHT), bovine serum albumin and tetraethoxypropane were purchased from Sigma Chemical Company (St. Louis, MO, USA). The haematoxylin and eosin stain assay kit was purchased from Beyotime Institute of Biotechnology (Haimen, Jiangsu, China). The GSH-400 colorimetric assay kit was purchased from Jiancheng Bioengineering Institute (Nanjing, Jiangsu, China).

The SiO_2 nanoparticles (20 and 50 nm) used in this study were supplied by Laboratory for Ultrafine Materials (East China University of Science and Technology, Shanghai, China). The nanoparticles were suspending in deionized water, the stock concentration of SiO_2 was 10.0 mg/ml.

2.2. Cell culture

The HEK293 cell line was purchased from cell bank of Chinese Academy of Sciences (Shanghai, China). Cells were cultured in a full DMEM medium containing 10% FBS, 100 U/ml penicillin and 100 μg/ml streptomycin, and incubated at 37 °C in with 5% CO_2.

2.3. SiO_2 nanoparticles exposure

The stock suspensions of SiO_2 nanoparticles were sterile filtered and stored at 4 °C. In each study, the stock suspensions were freshly diluted to different concentrations in the cell culture medium. After cells had attached for 12 h in the full medium, the medium was replaced with low serum DMEM (containing 0.1% FBS) to prevent particle agglomeration. Freshly dispersed particle suspensions were immediately applied to the cells. Cells free of SiO_2 nanoparticles were used as control cells throughout each assay.

2.4. Assessment of cytotoxicity

Mitochondrial function and cell viability were measured by the MTT assay (Denizot and Lang, 1986). HEK293 cells were plated into a 96-well plate at a density of 1.0×10^4 cells/well. Cells were grown overnight in the full medium and then switched to the low serum media followed by exposure to SiO_2 nanoparticles. Following the treatment, the cells were incubated with MTT (0.5 mg/ml) for 4 h. The medium was then removed and 100 μl of DMSO were added into each well to dissolve formazan crystals, the metabolite of MTT. After thoroughly mixing, the plate was read at 570 nm for optical density that is directly correlated with cell quantity. Survival rate was calculated from the relative absorbance at 570 nm and expressed as the percentage of control. Dose- and time-dependency of cellular toxicity were plotted from MTT results.

2.5. Qualitative observation of cellular morphology

The haematoxylin and eosin stain assay kit was used for the morphology observation of HEK293 cells. HEK293 cells were plated into a 24-well plate at a density of 1.0×10^5 cells/well. Following treatment described in the previous section, the cells were washed in ice-cold phosphate buffered saline (PBS) and fixed with 10% paraformaldehyde. The cells were then stained with haematoxylin and eosin to improve visualization and were observed under an XSP-17C contrast inverted microscopy (Changfang Optical Instruments, China).

2.6. Intracellular ROS measurement

The production of intracellular ROS was measured using DCFH–DA (Wang and Joseph, 1999). DCFH–DA passively enters the cell, where it reacts with ROS to form a highly fluorescent compound, dichlorofluorescein (DCF). Briefly, a DCFH–DA stock solution (10 mM in methanol) was diluted 1000-fold in DMEM without serum to yield a 10 μM working solution. HEK293 cells were plated into a 96-well plate at a density of 1.0×10^4 cells per well. After 24 h exposure to SiO_2 nanoparticles, the cells were washed twice with PBS and then incubated in 2 ml working solution of DCFH–DA at 37 °C for 30 min. Fluorescence was then determined at 485 nm excitation and 525 nm emission using a Bio-Tek Synergy HT-I plate reader (Bio-Tek Instruments, USA).

2.7. Quantification of intracellular GSH levels

Cellular levels of reduced GSH were determined using the GSH-400 colorimetric assay kit. The method is based on a chemical reaction between GSH and 5,5′-dithiobis (2-nitrobenzoic acid) (DTNB) to generate glutathione disulfide (GSSG) and -nitro-5-thiobenzoic acid, a yellow colored product. Thus GSH concentration in a sample solution can be determined by the measurement at 412 nm absorbance (Akerboom and Sies, 1981). HEK293 cells were plated into a 24-well plate at a density of 1.0×10^5 cells/well. After 24 h exposure to SiO_2 nanoparticles, the cells were washed twice in ice-cold PBS and then homogenized in 400 μl of 0.5% Triton X-100. The cell homogenate was centrifuged at 3000*g* at 4 °C for 10 min. The assay was performed on 200 μl centrifugation supernatants according to manufacturer's protocol, and the absorbance of the supernatant was measured at 400 nm using a UV-7500 UV–visible Spectrophotometer (Keda Instruments, China). Protein content was determined for

the same cell homogenate. GSH level was calculated from the absorbance at 400 nm and expressed as the percentage of control.

2.8. Estimation of lipid peroxidation

The MDA content, a measure of lipid peroxidation, was assayed in the form of thiobarbituric acid reactive substance (TBARS) (Ohkawa et al., 1979). HEK293 cells were plated into a 24-well plate at a density of 1.0×10^5 cells/well. After 24 h exposure to SiO_2 nanoparticles, the cells were washed with ice-cold PBS and homogenized in 400 μl of 0.5% Triton X-100. The cell homogenates were used in the TBARS assay. Briefly, 100 μl cell homogenates were mixed with 1 ml of 0.67% TBA, 1.5 ml 20% trichloroacetic acid, and 1.5 ml 0.04% BHT in test tubes. The mixtures were incubated in a boiling water bath for 20 min. After cooling to room temperature, the reaction mixture was centrifuged at 4000*g* for 10 min and the absorbance of the supernatant was measured at 532 nm using the same UV–visible Spectrophotometer. The concentrations of TBARS were calculated using tetraethoxypropane as a reference standard. Protein content was determined for the same cell homogenate. The quantities of TBARS were presented as the percentage of TBARS production over the control.

2.9. Flow cytometric analysis of cellular DNA content

It is well established that DNA fragmentation during apoptosis may lead to extensive loss of DNA content and result in a distinct sub-*G*1 peak when cells are analyzed by flow cytometry (Tuschl and Schwab, 2004). Flow cytometric analysis of cellular DNA content was performed as described previously (Liu et al., 2008). HEK293 cells were seeded in a six-well culture plate at a density of 2.0×10^5 cells/well. After the SiO_2 treatments, the cells were collected, fixed and permeabilized with 75% ice-cold ethanol overnight at 4 °C. The cells were then washed with PBS and resuspended in 1 ml of lysis buffer (0.1% Triton X-100, 0.05 mg/ml propidium iodide, and 1 mg/ml RNase A). After incubation for 30 min at 37 °C, the cells were analyzed analyzed in a FACScan flow cytometer (Becton Dickinson, USA) at 488 nm excitation and 620 nm emission. The percentage of cells in *G*0/*G*1 phase, *S* phase, *G*2/*M* and sub-*G*1 phase was analyzed using standard ModiFit and CellQuest software programs.

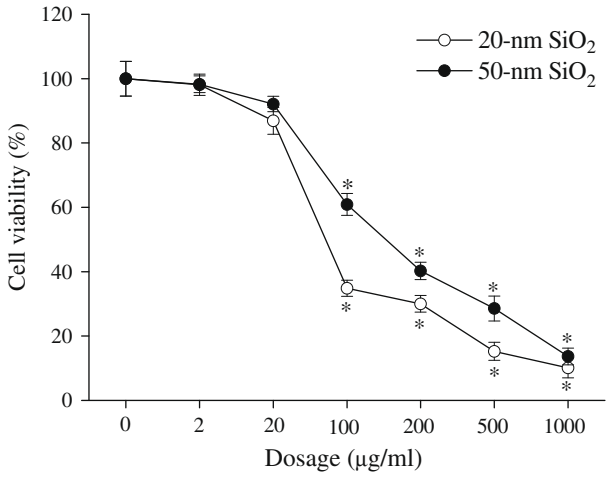

Fig. 1. Dose-dependent toxicity of 20 and 50 nm SiO_2 nanoparticles in HEK293 cells. Cells were treated with various concentrations of SiO_2 nanoparticles for 24 h and the viability was determined by MTT assay. Control cells cultured in nanoparticle-free medium were run in parallel to the treated groups. Values were the mean ± SD from three independent experiments. Significance indicated by: * $p < 0.05$ versus control cells.

2.10. Protein assay

The total protein concentration was measured by the Bradford method (Bradford, 1976) using bovine serum albumin as the standards.

2.10.1. Statistics

All data were reported as the mean ± standard deviation (SD). Statistical analysis was performed for the experiments conducted in at least triplicate using Student's *t*-test. Results with $p < 0.05$ were considered to be statistically significant.

3. Results

3.1. Dose-dependent cytotoxicity of SiO_2 nanoparticles

HEK293 cells were exposed to SiO_2 nanoparticles (20 and 50 nm) at 2, 20, 100, 200, 500, and 1000 μg/ml for 24 h. Cell viability decreased as a function of dosage levels (Fig. 1) Significant differences were seen from the 20 nm group treated at the concentrations of 100, 200, and 500 μg/ml. Both 20 and 50 nm

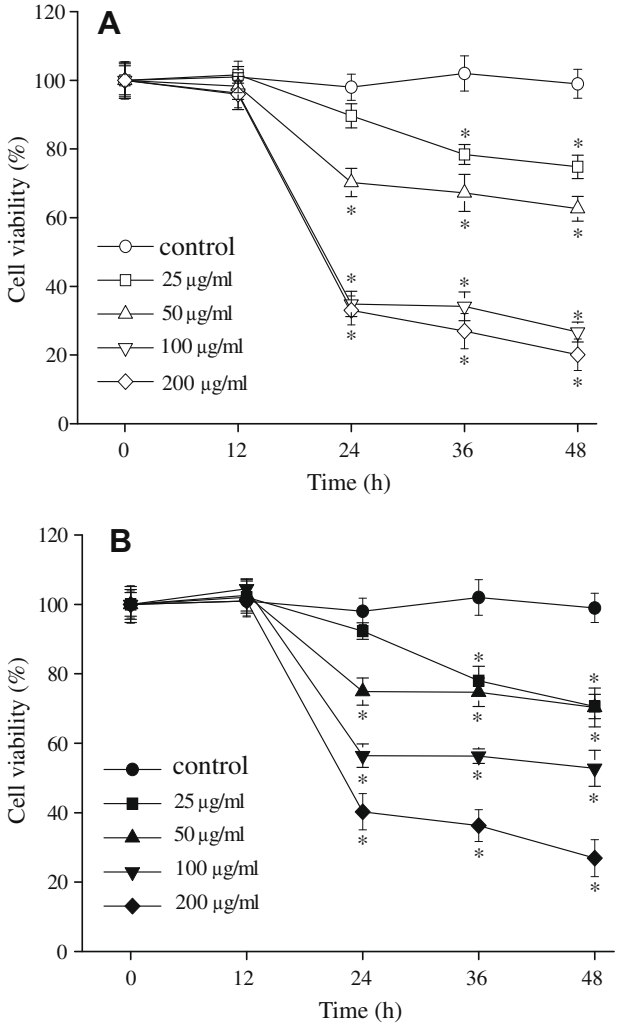

Fig. 2. Time-dependent toxicity of 20 and 50 nm SiO_2 nanoparticles in HEK293 cells. Cells were treated with 25, 50, 100, 200 μg/ml of SiO_2 nanoparticles for 12, 24, 36, and 48 h. Control cells cultured in nanoparticle-free medium were run in parallel to the treated groups. The viability was determined by MTT assay at different time points. (A) The 20 nm groups; (B) the 50 nm groups. Values were the mean ± SD from three independent experiments. Significance indicated by: * $p < 0.05$ versus control cells.

nanoparticles showed significantly cytotoxicity at concentrations above 20 μg/ml. The LD_{50} values obtained after 24 h exposure were 80.2 ± 6.4 μg/ml for 20 nm SiO_2 and 140.3 ± 8.6 μg/ml for 50 nm SiO_2 nanoparticles, respectively.

3.2. Time-dependent cytotoxicity of SiO_2 nanoparticles

HEK293 cells were exposed to SiO_2 nanoparticles (20 and 50 nm) at 25, 50, 100, and 200 μg/ml for 12, 24, 36, and 48 h. Cell viability decreased as a function of both time and dose (Fig. 2). At the dosage of 25 μg/ml, cell viability gradually decreased as the exposure time increased. At the doses of 50, 100, and 200 μg/ml, significant differences in cell viability were observed after 24 h exposure (Fig. 2A and B).

Based on the dose- and time-dependent studies, a dosage level lower than 20 μg/ml did not show significant cytotoxicity in HEK293 cells whereas a dosage level higher than 100 μg/ml resulted in severe precipitation of the nanoparticles in the cell media after 48 h. Therefore, the dosage range of 20–100 μg/ml of SiO_2 nanoparticles and 24 h exposure were selected for further studies.

3.3. Effect of SiO_2 nanoparticles on cellular morphology

HEK293 cells were exposed to SiO_2 nanoparticles (20 and 50 nm) for 24 h and morphological changes were examined using phase-contrast microscopy. Fig. 3A showed the morphology of control cells. Significant morphological changes in HEK293 cells were observed after SiO_2 nanoparticle exposure charactering the features of apoptosis such as cell shrinkage, irregular shapes, and nuclear condensation (Fig. 3B and D). The 20 nm SiO_2 nanoparticles seemed to be more cytotoxic than did the 50 nm SiO_2 nanoparticles. Size- and dose-dependent cytotoxic effects were well demonstrated (Fig. 3).

3.4. Effect of SiO_2 nanoparticles on ROS production

The fluorescence intensity of DCF, an indication of oxidative stress in suffered cells, increased after 24 h exposure to 20 and 50 nm SiO_2 nanoparticles at all concentrations examined. The ROS production was SiO_2 concentration dependent. Compared to the controls, DCF-fluorescence intensity increased by 26.6%,

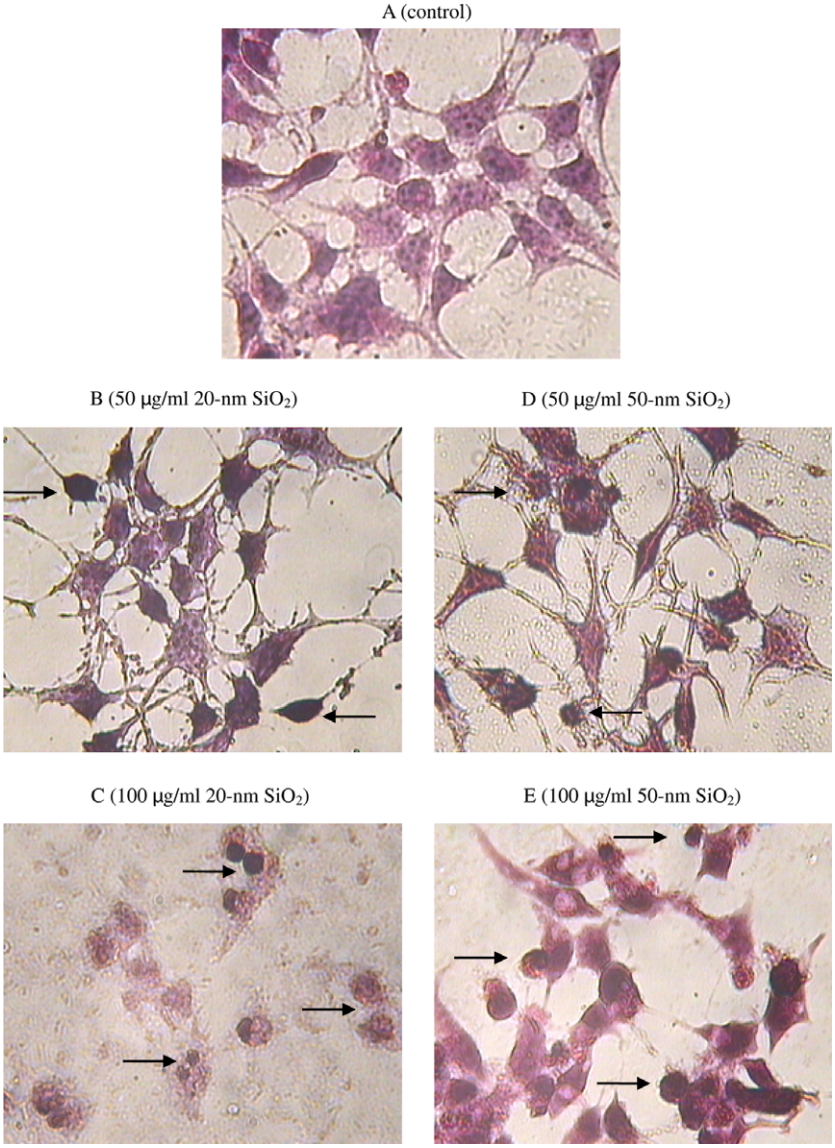

Fig. 3. Morphological characterization of HEK293 cells. Cells were exposed to different concentrations of SiO_2 nanoparticles for 24 h and stained with haematoxylin and eosin. The slides were visualized under an inverted microscope (magnification 250×). Arrow: cells with nuclear condensation and irregular shapes (in D and B), or apoptotic cells (in E and F).

82.7%, and 126.1% after exposure to 20 nm SiO_2 nanoparticles at 25, 50, and 100 μg/ml, respectively (Fig. 4). Compared to the ROS generated from the 20 nm group, less amounts of the ROS were detected in the cells treated with the 50 nm SiO_2 nanoparticles.

3.5. Effect of SiO_2 nanoparticles on intracellular GSH levels

GSH is a ubiquitous sulfhydryl-containing molecule in cells that is responsible for maintaining cellular oxidation–reduction homeostasis. Alterations in GSH homeostasis can be considered as an indication of functional-damage to the cells. Both SiO_2 nanoparticles (20 and 50 nm) decreased GSH levels in the cells. A partial decrease of GSH was already detectable at 25 μg/ml of 20 nm SiO_2 (16.4 ± 3.6%). When the dose increased to 100 μg/ml the intracellular GSH was almost reduced by half (52.1 ± 4.1%) compared to the control (Fig. 5). Overall, the data demonstrated a significant depletion of GSH levels in SiO_2 nanoparticles exposed cells. There was a significant reverse-correlation between ROS levels and GSH levels (R^2 = 0.981) (Fig. 6).

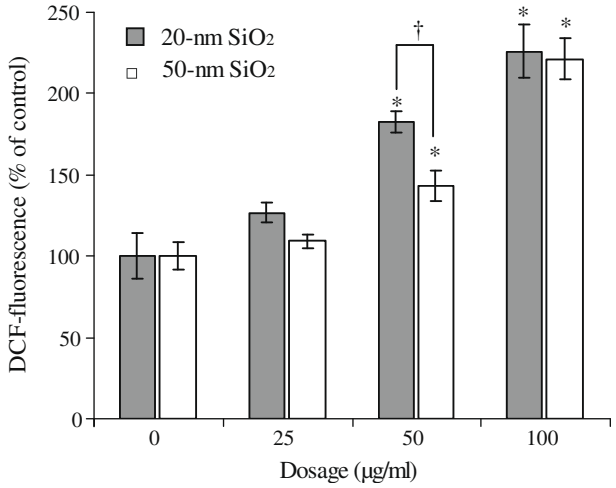

Fig. 4. DCF-fluorescence intensity in HEK293 cells after 24 h exposure to 25, 50, or 100 μg/ml of 20 and 50 nm SiO_2 nanoparticles. Values were the mean ± SD from three independent experiments. Significance indicated by: $^{*}p < 0.05$ versus control cells; †$p < 0.05$ versus cells exposed to 50 nm SiO_2 nanoparticles.

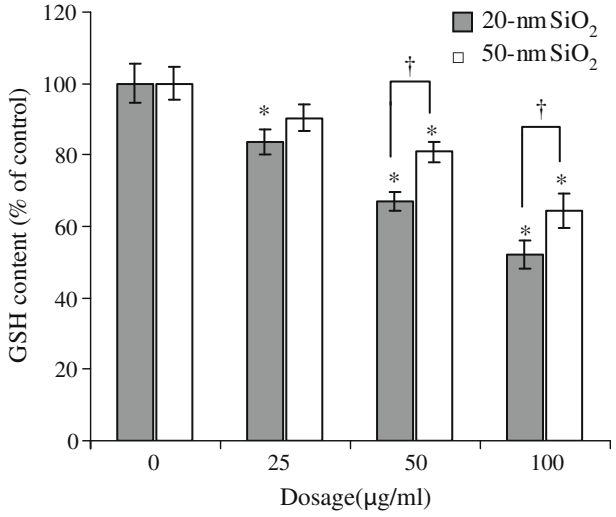

Fig. 5. Effect of 20 and 50 nm SiO_2 nanoparticles on GSH levels in HEK293 cells. Cells were treated with different concentrations of SiO_2 nanoparticles for 24 h. At the end of the exposure, cells were washed with PBS and GSH levels (control: 34.3 ± 2.3 nmol GSH/mg protein) were measured as described in Section 2. Control cells cultured in SiO_2-free medium were run in parallel to the treated groups. Values were the mean ± SD from three independent experiments. Significance indicated by: $^{*}p < 0.05$ versus control cells; †$p < 0.05$ versus cells exposed to 50 nm SiO_2 nanoparticles.

3.6. Effect of SiO_2 nanoparticles on lipid peroxidation

The sensitivity of measuring TBARS has made the assay the method of choice for screening and monitoring lipid peroxidation, a major indicator of oxidative stress. As showed in Fig. 7, both sizes of SiO_2 nanoparticles increased TBARS levels in HEK293 cells and 20 nm SiO_2 particles showed more significant effects. A reverse linear correlation was observed between TBARS content and cell viability (R^2 = 0.971) in Fig. 8, and a similar reverse correlation was observed between ROS levels and cell viability (R^2 = 0.956).

3.7. Effect of SiO_2 nanoparticles on cell cycle distribution

After 24 h exposure to 20 or 50 nm SiO_2 particles, cell cycle distribution was measured using flow cytometry. As shown in Table 1,

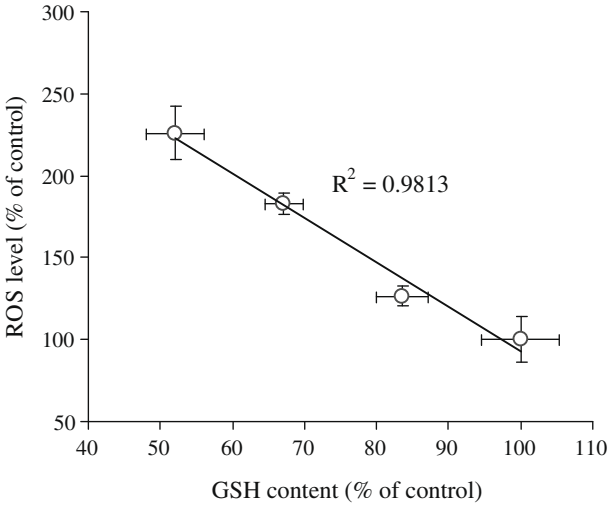

Fig. 6. Correlation between ROS levels and GSH levels after 24 h exposure to 25, 50, and 100 μg/ml of 20 nm SiO_2 nanoparticles.

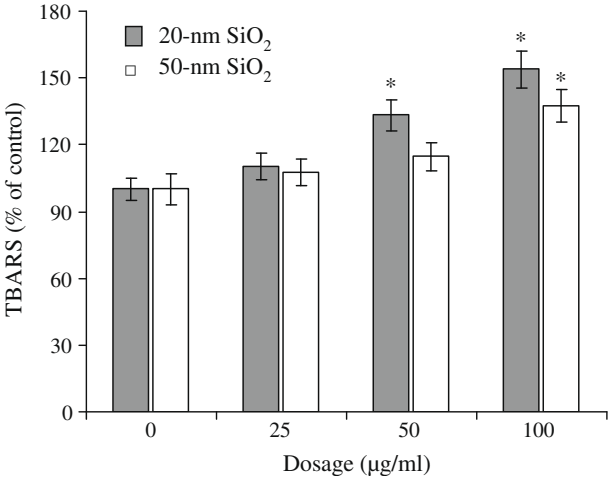

Fig. 7. Cellular TBARS levels of HEK293 cells after 24 h exposure to 20 and 50 nm SiO_2 nanoparticles. Control cells cultured in nanoparticle-free medium were run in parallel to the treated groups (control: 5.3 ± 0.2 nmol TBARS/mg protein). Values were mean ± SD from three independent experiments. Significance indicated by: $^{*}p < 0.05$ versus control cells; †$p < 0.05$ versus cells exposed to 50 nm SiO_2 nanoparticles.

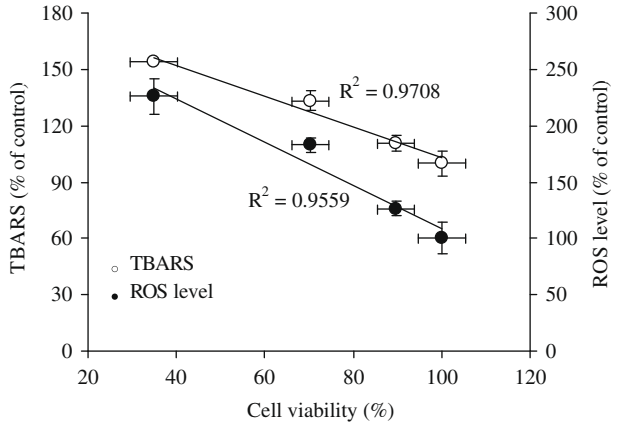

Fig. 8. Correlation between cell viability versus TBARS content, and ROS level after 24 h exposure to 25, 50, or 100 μg/ml of 20 nm SiO_2 nanoparticles.

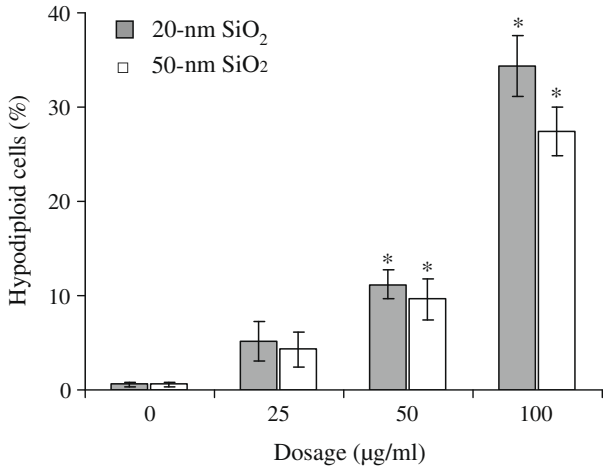

Fig. 9. The percentage of hypodiploid cells after 24 h exposure to 20 and 50 nm SiO_2 nanoparticles. HEK293 cells were exposed to different doses of SiO_2 nanoparticles for 24 h, then cells were harvested and stained with propidium iodide. Hypodiploid cells with DNA content less than *G*1 in the cell cycle distribution were counted as apoptotic cells by flow cytometric analysis. Values were mean ± SD from three independent experiments. Significance indicated by: * $p < 0.05$ versus control cells.

an induction of cell cycle transition from phase *G*0/*G*1 to phase *G*2/*M* was observed, with no significant change in the proportion of cells in phase *S*. An exposure of cells to 50, 100 μg/ml 20 nm SiO_2 for 24 h resulted in the accumulation of *G*2/*M* phase, from 8.9%(control) to 13.9% and 38.7%, respectively. These results suggested that SiO_2 nanoparticles inhibited the cellular proliferation via *G*2/*M* phase arrest in a dose-dependent manner.

3.8. Effect of SiO_2 nanoparticles on apoptotic sub-G1 population

Hypodiploid cells with DNA content less than *G*1 in the cell cycle distribution were counted as apoptotic cells by flow cytometric analysis. The sub-*G*1 population in SiO_2-exposed groups increased with the increment in the dosage of nanoparticles (Fig. 9). The percentage of hypodiploid cells was 5.1%, 11.2% and 34.4% after exposure to 20 nm SiO_2 nanoparticles at 25, 50, and 100 μg/ml, respectively. The 20 nm SiO_2 induced more sub-*G*1 fraction than 50 nm SiO_2 at the three exposure dosages.

4. Discussion

The purpose of this investigation was to evaluate potential toxicity and the general mechanism involved in nanoparticle-induced cytotoxicity. In this study, the cytotoxicity of two sizes of SiO_2 nanoparticles (20 and 50 nm) was investigated in cultured human embryonic kidney cells.

In the present study, it was found that exposure to SiO_2 nanoparticles at dosage levels of 20–100 μg/ml caused both dose- and time-dependent cytotoxicity as revealed by MTT assay and cell morphology study. It is generally perceived that the smaller the particle, the greater its toxicity (Kipen and Laskin, 2005; Oberdorster et al., 2005; Nel et al., 2006). Because of the larger specific surface area and the easier penetration into the cells, the 20 nm SiO_2 particles induced more significant cytotoxicity than did the 50 nm SiO_2 particles as expected.

Concomitant cellular oxidative stress was manifested by elevated ROS levels, reduced GSH levels, and increased lipid peroxidation. The inverse linear relationship between the ROS level and the GSH level indicated that free radical species were generated by exposure to SiO_2 nanoparticles which reduced intracellular antioxidant levels ($R^2 = 0.981$). Moreover, free radicals also resulted in the production of malondialdehyde, an indication of lipid peroxidation. There was a strong correlation between decreased cell viability and increased ROS level after 24 h exposure ($R^2 = 0.956$). The reverse-correlation between the decreased cell viability and the increased TBARS suggested that cell death was the primary cause of the membrane damage by lipid peroxidation. Lactate dehydrogenase leakage form cells are another evidence for penetration of particles into the cells and cell membrane damage (Balduzzi et al., 2004; Sayes et al., 2005). It has been well documented that lactate dehydrogenase levels (as a marker of necrosis) in the cell medium elevated after the cells exposed to nanoparticles (Hussain et al., 2005; Lin et al., 2006). However, in this study, most of the cells exposed to SiO_2 nanoparticles showed cell shrinkage and nuclear condensation, which are important markers of apoptosis. Flow cytometric analysis showed that SiO_2 nanoparticles can cause *G*2/*M* phase arrest in a dose-dependent manner, and subsequently the apoptotic sub-*G*1 phase increased obviously after 24 h exposure, suggesting the sequential events of cell cycle arrest followed by apoptosis.

Several mechanisms have been proposed to explain the adverse health effects of particulate pollutants. ROS production and the generation of oxidative stress have received the most attention. ROS, such as superoxides, hydrogen peroxide, hydroxyl and other oxygen radicals, are capable of directly oxidizing the DNA, proteins, and lipids (Yoshida et al., 2004). There are many evidences showing that nanoparticles increase ROS production and can cause cell death in different types of cultured cells (Becker et al., 2002; Peters et al., 2007; Pulskamp et al., 2007; Park et al., 2008). Furthermore, it has been well documented that GSH depletion and ROS produc-

Table 1
Cell cycle distribution of SiO_2 nanoparticle-exposed HEK293 cells.

SiO_2		Cell cycle phase (% of cells)		
Size (nm)	Dosage (μg/ml)	*G*0/*G*1	*S*	*G*2/*M*
20	0	69.3 ± 5.4	21.8 ± 4.5	8.9 ± 1.3
	25	62.5 ± 6.4	23.4 ± 3.9	14.1 ± 4.5
	50	61.8 ± 5.8*	24.3 ± 5.4	13.9 ± 5.9
	100	44.8 ± 6.5*	16.5 ± 6.8	38.7 ± 6.3*
50	25	65.0 ± 3.4	23.2 ± 1.9	11.8 ± 2.6
	50	63.7 ± 1.6	24.4 ± 2.8	11.9 ± 3.2
	100	58.1 ± 3.9	20.4 ± 3.7	21.5 ± 2.4*

After 24 h exposure to increasing doses of 20 or 50 nm SiO_2 nanoparticles, the HEK293 cells were harvested and analyzed for cell cycle and apoptosis using flow cytometry. The percent of cells in different cell phase was analyzed. Values were mean ± SD from three independent experiments.
* $p < 0.05$ versus control cells (cells free from SiO_2 nanoparticles).

tion cause mitochondrial dysfunction and changes in expression of distinct genes and pathways related to inflammatory responses and apoptosis including MAPK/ERK kinase, NFκB, MIP-2, caspase-3, Bcl-2 (Driscoll, 2000; Fubini and Hubbard, 2003; Kharasch et al., 2006). Thus apoptosis initiated by silica may be the result of increased ROS production and GSH depletion, leading to mitochondrial dysfunction, DNA damage, increased gene expression of death receptors and/or their corresponding ligands. Further studies are needed to investigate the expression of genes in these signaling pathways in response to exposure to SiO_2 nanoparticles.

In summary, our preliminary data has suggested that exposure of SiO_2 nanoparticles leads to cellular morphological modifications, mitochondrial dysfunction, and oxidative stress as indicated by elevation of intracellular ROS and TBARS, as well as depletion of GSH, which triggers cell cycle arrest and apoptosis in a dose-dependent manner. Further studies are underway to investigate the molecular mechanisms of apoptosis involved in silica nanoparticle toxicity.

Acknowledgment

Financial support from the Shanghai nanotechnology Leading Academic Discipline projects (project no. 0752nm025) is gratefully acknowledged.

References

Akerboom, T.P.M., Sies, H., 1981. Assay of glutathione, glutathione disulfide, and glutathione mixed disulfides in biological samples. Methods Enzymol 77, 373–382.

Arts, J.H., Muijser, H., Duistermaat, E., Junker, K., Kuper, C.F., 2007. Five-day inhalation toxicity study of three types of synthetic amorphous silicas in Wistar rats and post-exposure evaluations for up to 3 months. Food and Chemical Toxicology 45, 1856–1867.

Balduzzi, M., Diociaiuti, M., De Berardis, B., Paradisi, S., Paoletti, L., 2004. In vitro effects on macrophages induced by noncytotoxic doses of silica particles possibly relevant to ambient exposure. Environmental Research 96, 62–71.

Barik, T.K., Sahu, B., Swain, V., 2008. Nanosilica-from medicine to pest control. Parasitology Research 103 (2), 253–258.

Becker, S., Soukup, J.M., Gallagher, J.E., 2002. Differential particulate air pollution induced oxidant stress in human granulocytes, monocytes and alveolar macrophages. Toxicology in Vitro 16, 209–218.

Bharali, D.J., Klejbor, I., Stachowiak, E.K., Dutta, P., Roy, I., Kaur, N., Bergey, E.J., Prasad, P.N., Stachowiak, M.K., 2005. Organically modified silica nanoparticles: a nonviral vector for in vivo gene delivery and expression in the brain. Proceedings of the National Academy of Sciences of the United States of America 102, 11539–11544.

Bradford, M.M., 1976. A rapid and sensitive method for the quantitation of microgram quantities of protein utilizing the principle of protein-dye binding. Analytical Biochemistry 72, 248–254.

Chang, J.S., Chang, K.L., Hwang, D.F., Kong, Z.L., 2007. In vitro cytotoxicity of silica nanoparticles at high concentrations strongly depends on the metabolic activity type of the cell line. Environmental Science and Technology 41, 2064–2068.

Chen, M., von Mikecz, A., 2005. Formation of nucleoplasmic protein aggregates impairs nuclear function in response to SiO_2 nanoparticles. Experimental Cell Research 305, 51–62.

Chen, J.M., Tan, M.G., Nemmar, A., Song, W.M., Dong, M., Zhang, G.L., Li, Y., 2006. Quantification of extrapulmonary translocation of intratracheal-instilled particles in vivo in rats: effect of lipopolysaccharide. Toxicology 222, 195–201.

Driscoll, K.E., 2000. TNFα and MIP-2: role in particle-induced inflammation and regulation by oxidative stress. Toxicology Letters 112–113, 177–184.

Denizot, F., Lang, R., 1986. Rapid colorimetric assay for cell growth and survival: modifications to the tetrazolium dye procedure giving improved sensitivity and reliability. Journal of Immunological Methods 89, 271–277.

Florea, A.M., Splettstoesser, F., Büsselberg, D., 2007. Arsenic trioxide (As_2O_3) induced calcium signals and cytotoxicity in two human cell lines: SY-5Y neuroblastoma and 293 embryonic kidney (HEK). Toxicology and Applied Pharmacology 220, 292–301.

Fubini, B., Hubbard, A., 2003. Reactive oxygen species and reactive nitrogen species generation by silica in inflammation and fibrosis. Free Radical Biology and Medicine 34, 1507–1516.

Gao, F., Horie, T., 2002. A synthetic analog of prostaglandin E1 prevents the production of reactive oxygen species in the intestinal mucosa of methotrexate-treated rats. Life Sciences 71, 1091–1099.

Gemeinhart, R.A., Luo, D., Saltzman, W.M., 2005. Cellular fate of a modular DNA delivery system mediated by silica nanoparticles. Biotechnology Progress 21, 532–537.

Hirsch, L.R., Stafford, R.J., Bankson, J.A., Sershen, S.R., Rivera, B., Price, R.E., Hazle, J.D., Halas, N.J., West, J.L., 2003. Nanoshell-mediated near infrared thermal therapy of tumors under magnetic resonance guidance. Proceedings of the National Academy of Sciences of the United States of America 100, 13549–13554.

Hussain, S.M., Hess, K.L., Gearhart, J.M., Geiss, K.T., Schlager, J.J., 2005. In vitro toxicity of nanoparticles in BRL 3A rat liver cells. Toxicology in Vitro 19, 975–983.

Ji, L.L., Chen, Y., Wang, Z.T., 2008. The toxic effect of pyrrolizidine alkaloid clivorine on the human embryonic kidney 293 cells and its primary mechanism. Experimental and Toxicologic Pathology 60, 87–93.

Kharasch, E.D., Schroeder, J.L., Bammler, T., Beyer, R., Srinouanprachanh, S., 2006. Gene expression profiling of nephrotoxicity from the sevoflurane degradation product fluoromethyl-2,2-difluoro-1-(trifluoromethyl)vinyl ether (“compound a”) in rats. Toxicological Sciences 90, 419–431.

Kipen, H.M., Laskin, D.L., 2005. Smaller is not always better: nanotechnology yields nanotoxicology. The American Journal of Physiology – Lung Cellular and Molecular Physiology 289, 696–697.

Kleinman, M.T., Araujo, J.A., Nel, A., Sioutas, C., Campbell, A., Cong, P.Q., Li, H., Bondy, S.C., 2008. Inhaled ultrafine particulate matter affects CNS inflammatory processes and may act via MAP kinase signaling pathways. Toxicology Letters 178, 127–130.

Komatsu, T., Tabata, M., Kubo-Irie, M., Shimizu, T., Suzuki, K., Nihei, Y., Takeda, K., 2008. The effects of nanoparticles on mouse testis Leydig cells in vitro. Toxicology in Vitro 22, 1825–1831.

Kreyling, W.G., Semmler, M., Erbe, F., Mayer, P., Takenaka, S., Schulz, H., Oberdorster, G., Ziesenis, A., 2002. Translocation of ultrafine insoluble iridium particles from lung epithelium to extrapulmonary organs is size dependent but very low. Journal of Toxicology and Environmental Health A 65, 1513–1530.

Lin, W.S., Huang, Y.W., Zhou, X.D., Ma, Y.F., 2006. In vitro toxicity of silica nanoparticles in human lung cancer cells. Toxicology and Applied Pharmacology 217, 252–259.

Liu, J.W., Xu, W., Li, C.L., Wu, H.Z., Liu, Y.W., 2008. Kaempferol-7-O-b-D-glucoside (KG) isolated from Smilax china L. rhizome induces G2/M phase arrest and apoptosis on HeLa cells in a p53-independent manner. Cancer Letters 264, 229–240.

Mitsikosta, F., Fornasier, M., Westerberg, G., 2008. Lysosomes and oxidative stress in aging and apoptosis. Biochimica et Biophysica Acta 1780, 1291–1303.

Miyazono, Y., Gao, F., Horie, T., 2004. Oxidative stress contributes to methotrexate-induced small intestinal toxicity in rats. Scandinavian Journal of Gastroenterology 39, 1119–1127.

Nel, A., Xia, T., Madler, L., Li, N., 2006. Toxic potential of materials at the nanolevel. Science 311, 622–627.

Nemmar, A., Hoylaerts, M.F., Hoet, P.H., Nemery, B., 2004. Possible mechanisms of the cardiovascular effects of inhaled particles: systemic translocation and prothrombotic effects. Toxicology Letters 149, 243–253.

Oberdorster, G., Oberdorster, E., Oberdorster, J., 2005. Nanotoxicology: an emerging discipline evolving from studies of ultrafine particles. Environmental Health Perspectives 113, 823–839.

Ohkawa, H., Ohishi, N., Yagi, K., 1979. Assay for lipid peroxides in animal tissues by thiobarbituric acid reaction. Analytical Biochemistry 95, 351–358.

Park, E.J., Choi, J., Park, Y., Park, K., 2008. Oxidative stress induced by cerium oxide nanoparticles in cultured BEAS-2B cells. Toxicology (1–2), 90–100.

Park, E.J., Park, K., 2008. Oxidative stress, pro-inflammatory responses induced by silica nanoparticles in vivo and in vitro. Toxicology Letters. doi:10.1016/j.toxlet.2008.10.012.

Peters, K., Unger, R.E., Kirkpatrick, C.J., Gatti, A.M., Monari, E., 2004. Effects of nano-scaled particles on endothelial cell function in vitro: studies on viability, proliferation and inflammation. Journal of Materials Science: Materials in Medicine 15, 321–325.

Peters, K., Unger, R.E., Gatti, A.M., Sabbioni, E., Tsaryk, R., Kirkpatrick, C.J., 2007. Metallic nanoparticles exhibit paradoxical effects on oxidative stress and pro-inflammatory response in endothelial cells in vitro. International Journal of Immunopathology and Pharmacology 20, 685–695.

Pisanic II, T.R., Blackwella, J.D., Shubayev, V.I., Finones, R.R., Jin, S.H., 2007. Nanotoxicity of iron oxide nanoparticle internalization in growing neurons. Biomaterials 28, 2572–2581.

Pulskamp, K., Diabate, S., Krug, H.F., 2007. Carbon nanotubes show no sign of acute toxicity but induce intracellular reactive oxygen species in dependence on contaminants. Toxicology Letters 168, 58–74.

Santra, S., Zhang, P., Wang, K., Tapec, R., Tan, W., 2001. Conjugation of biomolecules with luminophore-doped silica nanoparticles for photostable biomarkers. Analytical Biochemistry 73, 4988–4993.

Sayes, C.M., Gobin, A.M., Ausman, K.D., Mendez, J., West, J.L., Colvin, V.L., 2005. Nano-C60 cytotoxicity is due to lipid peroxidation. Biomaterials 26, 7587–7595.

Slowing, I.I., Vivero-Escoto, J.L., Wu, C.W., Lin, V.S.Y., 2008. Mesoporous silica nanoparticles as controlled release drug delivery and gene transfection carriers. Advanced Drug Delivery Reviews 60, 1278–1288.

Tuschl, H., Schwab, C.E., 2004. Flow cytometric methods used as screening tests for basal toxicity of chemicals. Toxicology in Vitro 18, 483–491.

Wang, H., Joseph, J.A., 1999. Quantitating cellular oxidative stress by dicholorofluorescein assay using microplate reader. Free Radical Biology and Medicine 27, 612–616.

Warheit, D.B., Hoke, R.A., Finlay, C., Donner, E.M., Reed, K.L., Sayes, C.M., 2007. Development of a base set of toxicity tests using ultrafine TiO_2 particles as a component of nanoparticle risk management. Toxicology Letters 171, 99–110.

Wick, P., Manser, P., Limbach, L.K., Weglikowska, U.D., Krumeich, F., Roth, S., Stark, W.J., Bruinink, A., 2007. The degree and kind of agglomeration affect carbon nanotube cytotoxicity. Toxicology Letters 168, 121–131.

Yoshida, Y., Itoh, N., Saito, Y., Hayakawa, M., Niki, E., 2004. Application of water-soluble radical initiator, 2,2-azobis[2-(2-imidazolin-2-yl)propane] dihydrochloride, to a study of oxidative stress. Free Radical Research 38, 375–384.

Zhang, F.F., Wan, Q., Li, C.X., Wang, X.L., Zhu, Z.Q., Xian, Y.Z., Jin, L.T., Yamamoto, K., 2004. Simultaneous assay of glucose, lactate, L-glutamate and hypoxanthine levels in a rat striatum using enzyme electrodes based on neutral red-doped silica nanoparticles. Analytical and Bioanalytical Chemistry 380, 637–642.